International Journal of Machine Tools & Manufacture 65 (2013) 99–106

Contents lists available at SciVerse ScienceDirect

International Journal of Machine Tools & Manufacture

journal homepage: www.elsevier.com/locate/ijmactool

Micro-cutting characteristics of EDM fabricated high-precision polycrystalline diamond tools

Zhiyu Zhang [a,b], Huanming Peng [b], Jiwang Yan [c,*]

[a] Changchun Institute of Optics, Fine Mechanics and Physics, Chinese Academy of Science, Dongnanhu Road 3888, Changchun, Jilin 130025, China
[b] Department of Mechanical Systems and Design, Graduate School of Engineering, Tohoku University, Aramaki Aoba 6-6-01, Aoba-ku, Sendai 980-8579, Japan
[c] Department of Mechanical Engineering, Faculty of Science and Technology, Keio University, Hiyoshi 3-14-1, Kohoku-ku, Yokohama 223-8522, Japan

ARTICLE INFO

Article history:
Received 8 July 2012
Received in revised form
25 October 2012
Accepted 29 October 2012
Available online 6 November 2012

Keywords:
Micro cutting
Micro end mill
Polycrystalline diamond
Electro discharge machining
Structured surface
Mold fabrication

ABSTRACT

To fabricate three-dimensional microstructures, such as micro dimples, micro grooves and micro channels, on ceramic mold materials, tool fabrication with super hard materials is an essential step. In this work, micro electro discharge machining (EDM) was used to fabricate high-precision polycrystalline diamond end mills. Form accuracy and edge sharpness in one micron level were achieved by utilizing electro discharge induced graphitization of diamond grains under extremely low discharge energy conditions. The cutting performance of the fabricated tools was examined by machining micro dimples and micro grooves on tungsten carbide mold substrates. Results showed that using the EDM-fabricated tools, ductile mode machining of tungsten carbide was realized with a surface finish of 2 nm R_a, which is comparable to that produced by polishing.

1. Introduction

In recent years, there is an increasing demand for manufacturing large-area surface microstructures, such as micro groove arrays, micro pyramid arrays, and micro lens arrays. These microstructured surfaces can be used in optical communication devises, flat panel displays, light emitting diode applications, and so on [1,2]. For example, a micro lens array with lens diameter of several tens micrometers can increase 15% of luminance in the backlighting module of liquid crystal displays [3]. Micro lens array with lens diameter of several hundred micrometers is used in the Shack–Hartmann wavefront sensor to divide the wavefront surface into a number of beamlets [4].

Microstructures on semiconductor substrates can be manufactured by silicon-based micro machining methods such as photolithography and etching technology [5]. As for viscoelastic materials, replication techniques, such as plastic injection molding and glass molding press, are effective for microstructure fabrication. In the replication processes, the fabrication of precision molding dies is a crucial issue. Tungsten carbide (WC) is a commonly used die material for molding glass aspherical lenses, although the precision micro machining of WC is still challenging. Ultrasonic vibration assisted diamond cutting has been attempted to machine microstructures on WC, but there are a few limitations such as low machining speed and vibration-induced surface texture changes [6].

An alternative method is the use of micro end milling, which has been widely used in machining microstructures and curved surfaces on metals [7,8]. However, most of the previously used end mills were made of WC [9–11], which cannot be applied to the machining of WC molding dies. Single crystalline diamond end mill has been recently attempted for generating microstructures, but when machining super hard materials, like silicon carbide, cleavage-induced edge chippings and flank wear occur [12]. From this aspect, polycrystalline diamond (PCD) might be better than single crystalline diamond as the tool material for machining WC molds.

However, the fabrication of PCD micro end mills is extremely difficult due to the material's high strength and high hardness. Conventional tool fabrication methods, such as grinding and polishing, are not applicable because of extremely low material removal rate, long processing time, as well as rapid wear of the grinding wheels and polishing heads [13]. As a recently focused method, electro discharge machining (EDM) provides an effective way to micro tool fabrication. EDM is a noncontact process without problems of mechanical stress, tool bending/breaking and chattering [14,15]. EDM has been used for producing WC micro end mills [16–21]. For example, Fleischer et al. fabricated a WC end mill with a diameter of 100 μm by using wire EDM [19], and Yan et al. fabricated WC micro end mills with 50 μm

* Corresponding author. Tel.: +81 45 566 1445; fax: +81 45 566 1995.
E-mail address: yan@mech.keio.ac.jp (J. Yan).

0890-6955/$ - see front matter © 2012 Elsevier Ltd. All rights reserved.
http://dx.doi.org/10.1016/j.ijmachtools.2012.10.007

diameter [20]. Egashira et al. reported the EDM fabrication of a WC tool with a diameter of 3 μm for micro drilling [21].

EDM fabrication of PCD tools has also been reported. For example, Masaki et al. fabricated a spherical PCD grinding tool (radius 800 μm) for glass micro grinding [22]. Minami et al. fabricated a semi-cylindrical PCD tool with a diameter of 60 μm by EDM [23]. These studies have demonstrated the feasibility of shaping PCD tools by using micro EDM. However, little attention has been paid on tool precision. Normally, an EDM fabricated tool has low form accuracy, a rough surface finish and a dull edge due to the electro discharge-induced crater generation. To date, the cutting performance of an EDM fabricated tool has not yet been experimentally confirmed.

In this work, we explore the feasibility of fabricating high-precision micro PCD end mills by minimizing the crater size in micro EDM. In previous works, electro discharge pulse duration has been used as a controlling parameter for improving tool surface quality [23]. In this work, we use electro discharge energy to control material removal mechanism of PCD and to achieve high tool accuracy and edge sharpness. The cutting performance of the EDM fabricated PCD end mill was then examined by generating micro dimples and micro grooves on WC mold substrates.

2. Experiments

2.1. EDM fabrication of PCD end mills

2.1.1. Tool shape

To generate micro dimples for lens array applications, in the present work, single flute spherical micro end mill was considered. The rake face of the end mill is a flat surface (nominal rake angle 0°), and flank face is a hemispherical surface (nominal relief angle 0°). When using the tool for machining, hybrid effects maybe expected: one is cutting effect by the rake face, and the other is grinding effect by the diamond grains on the flank face. The former takes place at a large depth of cut (for rough machining) while the latter is dominant at a small depth of cut (for fine finishing).

Fig. 1 schematically shows shape generation method for end mills by wire EDM. The wire electrode is fed continuously by a wire guider, while the PCD tool electrode is kept rotating and feeding along the *X* and *Z* directions. As electro discharges occur at an extremely small area between the wire and the PCD tool, high-precision shape formation can be realized.

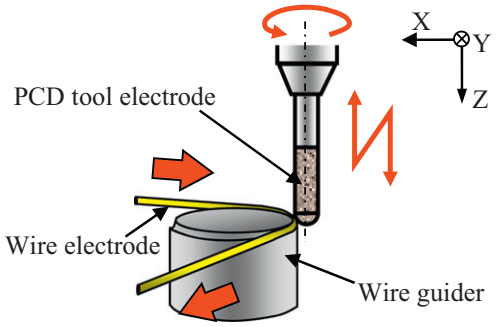

Fig. 1. Schematic of tool shape generation.

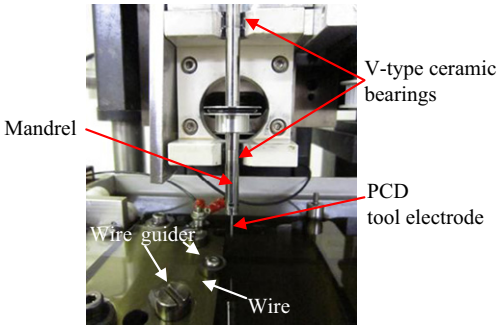

Fig. 2. Photograph of EDM setup.

2.1.2. EDM machine

Tool fabrication was performed by using a precision micro EDM machine, Panasonic MG-ED82W, which enables wire electro discharge grinding (WEDG) [17]. Fig. 2 shows a photograph of the main part of the machine. A PCD rod is clamped by a cylindrical mandrel which is supported by two V-type ceramic bearings on *Z*-axis table. This clamping mechanism is designed to minimize decentering errors caused by mounting and detaching of the tool electrode. The mandrel is driven by a DC motor at a rotation rate of 3000 rpm. A steel ball, rather than a motor brush, is used for providing an electrical connection between the mandrel and the electro discharge circuit.

Resistor-capacitor (RC) discharge circuit, as schematically shown in Fig. 3, is used in the machine. The discharging energy

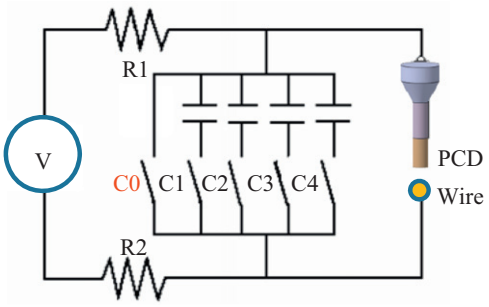

Fig. 3. Schematic of RC circuit for micro EDM.

Table 1
Experimental conditions for fabrication of PCD end mill.

Tool electrode material	Poly crystalline diamond		
Tool electrode rotation [rpm]	3000		
Wire electrode material	Brass		
Wire electrode diameter [μm]	100		
Voltage [V]	−110	−80	−70
Condenser capacitance [pF]	3300	10	1

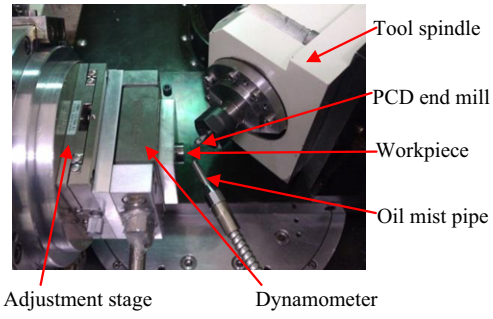

Fig. 4. Experimental setups used for micro end milling.

can be changed by adjusting the voltage (0–110 V), and/or the electrical capacitance of the RC circuit. The electrical capacitance is determined by condensers C1–C4 the capacities of which are 3300, 220, 100 and 10 pF, respectively.

2.1.3. EDM conditions

The PCD rod contains fine diamond grains having a mean size of 0.5 μm and a concentration of ~90%, with cobalt as binder. This grain size is remarkably smaller than those used in previous studies (~25 μm [21]). Table 1 shows experimental conditions for fabricating PCD end mills. A kind of commercially available EDM oil, Casty Lube EDS (Nikko Casty Co., Ltd.), was used as dielectric fluid. The polarity of PCD tool electrode was positive. The electro discharging energy was changed by adjusting discharging voltage and condenser capacitance. To realize extremely low discharging energy, in this work, we attempted to use the stray capacitance of the circuit C0 (~1 pF) instead of the condensers C1–C4. This enables electro discharging at an extremely low energy level. The discharging energy was set to three levels: 1.8×10^{-4} J (−110 V, 3300 pF) for rough machining, 3.2×10^{-8} J (−80 V, 10 pF) for semi-fine machining, and 2.5×10^{-9} J (−70 V, 1 pF) for fine machining, respectively.

The EDM fabricated end mills were examined by a scanning electron microscope (SEM), SU1510 (Hitachi, Co., Ltd.), and a non-contact laser-probe profilometer NH-3SP (Mitaka Kouki Co., Ltd.). To characterize tool material structural changes during EDM, a laser micro-Raman spectrometer NRS-3100 (JASCO Corporation, Japan) was used to analyze the tool surface.

Table 2
Experimental conditions for micro end milling of tungsten carbide.

Workpiece	Tungsten carbide
Radius of end mill [μm]	400
Tool spindle rotation [rpm]	10,000
Depth of dimple [μm]	25
Feed rate [mm/min]	0.1
Cutting environment	Oil mist

2.2. Micro cutting tests using the EDM fabricated tools

To evaluate cutting performance of the EDM fabricated tools, micro dimples and micro grooves were cut on a WC mold substrate. A three-axis (XZB) numerically controlled ultraprecision lathe Nachi-ASP15 (Fujikoshi Co. Ltd.) was used. Fig. 4 shows a photograph of the main section of the machine. The EDM fabricated end mill was fixed on a high-speed air spindle. A piezoelectric dynamometer, Kistler 9256 A, was mounted under the workpiece to measure machining forces. The machining conditions are shown in Table 2. Cutting oil Bluebe #LB10 was used as coolant by means of

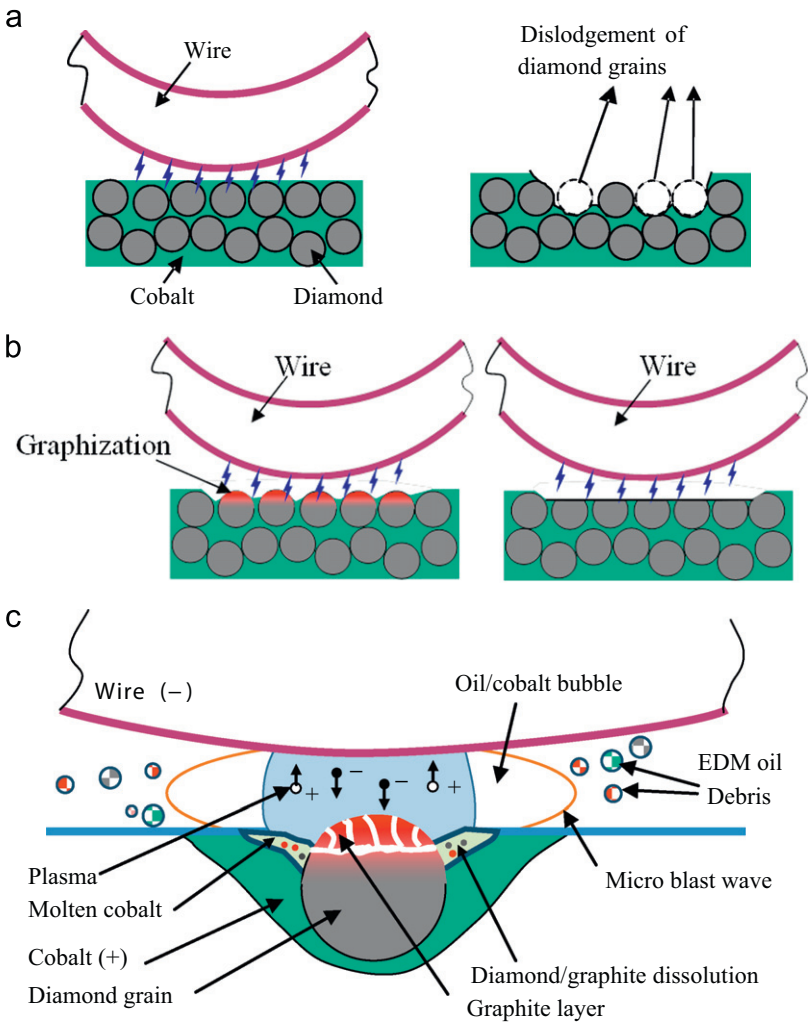

Fig. 5. Schematic models for material removal and surface generation in EDM of PCD under (a) high electro discharge energy condition, (b) low electro discharge condition; (c) is a detailed diagram showing graphitization, dissolution and gradual removal of a diamond grain.

mist jetting. The machined surfaces and collected cutting chips were examined using the SEM, and the surface roughness was measured by a white light interferometer Zygo NiewView 5000.

3. Results and discussion

3.1. EDM mechanism of PCD

It has been known that material removal in EDM of conductive metals occurs in a complex way involving melting, evaporation, oxidization, and chemical reaction [24,25]. However, to date, there is little literature on the EDM mechanism of PCD. Normally, EDM of PCD is performed at high discharge energy conditions to improve material removal rate. In this case, the electrically conductive binder (cobalt) is readily removed by melting and evaporation, while the nonconductive diamond grains fall off from the surface when losing the binding force, as schematically shown in Fig. 5(a). This kind of material removal will lead to surface roughening and is not suitable for high-precision tool fabrication.

In this work, we attempt to use an extremely low electro discharging energy to suppress the removal rate of cobalt binder and to enable gradual removal of diamond grains. In this case, as schematically shown in Fig. 5(b), we expect that microstructural changes of diamond, such as graphitization and thermochemical reactions, take place instead of grain falling off.

Breusov et al. [26] and Fedoseev et al. [27] found that in vacuum environment, graphitization of diamond occurs in a temperature range of 970–1670 K. Everson et al. [28] found that molten cobalt could significantly reduce the graphitization temperature of diamond. Qian et al. [29] demonstrated that diamond transformed into diamond-like carbon (amorphous) and graphite in a temperature range of 1500–2300 K.

In this paper, we estimated the maximum temperature $T(z)$ in micro EDM according to the anode erosion model proposed by Eubank et al. [30] and Yeo et al. [31]:

$$\left\{ \begin{array}{l} T(z) = \frac{2q\sqrt{\alpha t}}{k}\left[ierfc\left(\frac{z}{2\sqrt{\alpha t}}\right) - ierfc\left(\frac{\sqrt{z^2+r^2}}{2\sqrt{\alpha t}}\right)\right] \\ q = \frac{fp}{\pi r^2} \end{array} \right\} \quad (1)$$

where q is power flux, p pulse power, f fraction of pulse power expended at the anode, r radius of the circular spark channel, t pulse on-time, k thermal conductivity of work material, α thermal diffusivity, and $ierfc(x)$ integral complementary error function. The calculated maximum temperature is 5700 K, which is in accordance with the experimentally measured results (4000–11000 K) by Nagahanumaiah et al. [32], Kojima et al. [33], and Natsu et al. [34].

From this result, we can see that the temperature in electrical discharge region is sufficiently high to cause microstructural changes in diamond, such as graphitization and amorphization. Also, an extremely thin layer of diamond/graphite may directly dissolve into molten cobalt, like that in sintering process of PCD (~1700 K) [35,36]. Finally, the molten cobalt and the soft graphite layer can be removed easily by local micro blasts formed by

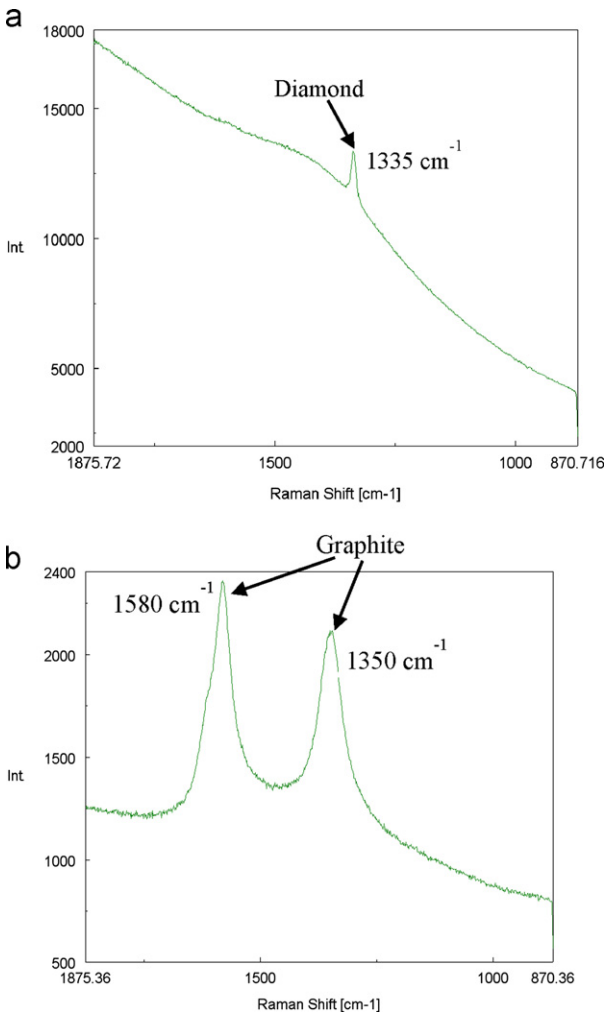

Fig. 6. Raman spectra of (a) as-received PCD rod, and (b) EDM finished PCD surface under fine machining conditions.

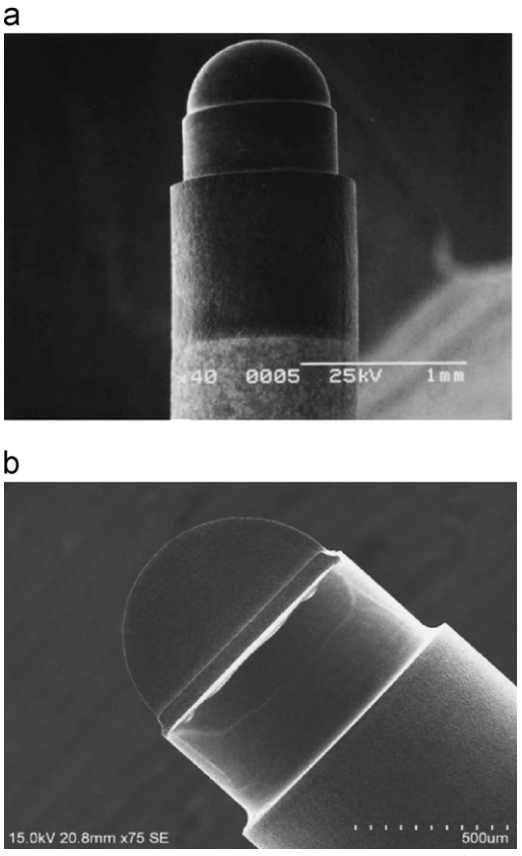

Fig. 7. SEM micrographs of EDM fabricated PCD tools: (a) hemispherical tool, (b) end mill.

vaporization of EDM oil. The aforementioned material removal mechanisms of PCD in EDM can be schematically shown in Fig. 5(c).

In this way, a very smooth surface will be obtained without crater generation. Therefore, by controlling surface graphitization of diamond grains, it should be possible to obtain an extremely smooth tool face and an extremely sharp tool edge in micro EDM of PCD tools. To verify the microstructural changes of diamond during EDM, we performed laser micro-Raman tests on the PCD tools.

Fig. 6(a) shows Raman spectra of an as-received PCD rod. There is a sharp peak at 1332 cm^{-1} that corresponds to the first order Raman peak of crystalline diamond. Fig. 6(b) shows result of an EDM finished PCD surface under fine machining conditions. In this case, there are two peaks at 1580 and 1350 cm^{-1}, respectively. The sharp peak at 1580 cm^{-1} (G band) indicates crystalline graphite, and the band at around 1350 cm^{-1} (D band) corresponds to microcrystalline graphite [37]. From this result, we may conclude that under low electro discharge energy conditions, diamond-graphite phase transformation takes place during micro EDM of PCD.

3.2. PCD tool fabrication

Under the conditions described above, we test fabricated a few micro PCD end mills. Fig. 7 shows SEM micrographs of a PCD hemispherical tool and a further shaped end mill, respectively. The flat surface crossing the center of the hemisphere serves as tool rake face, while the residual spherical surface serves as tool flank face.

Fig. 8 shows SEM micrographs of the edge and the flank face of an end mill obtained under rough machining conditions. Both the edge and the tool face are very rough with deep craters. This indicates that due to the high electro discharge energy, dislodgements of diamond grains occurred significantly during EDM. Fig. 9 shows SEM micrographs of the tool edge and the tool flank face obtained under fine machining conditions. In this case, however,

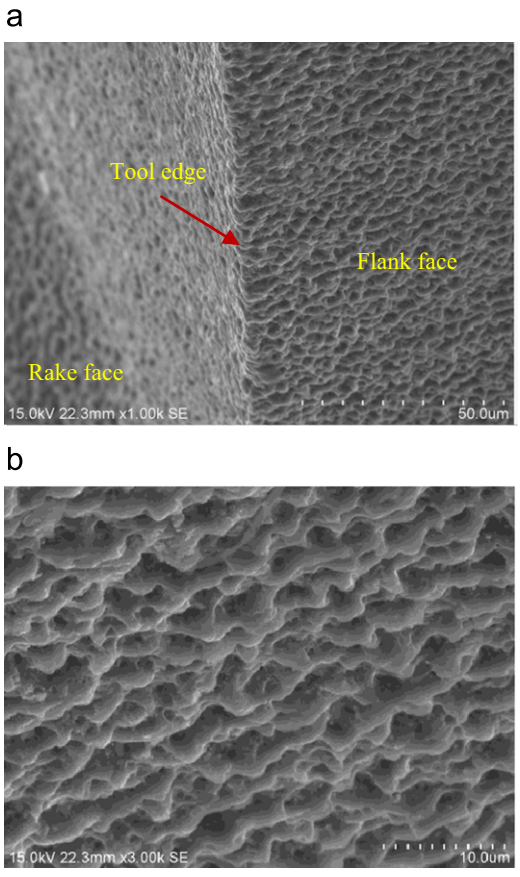

Fig. 8. SEM micrographs of (a) tool edge and (b) tool flank face in rough machining.

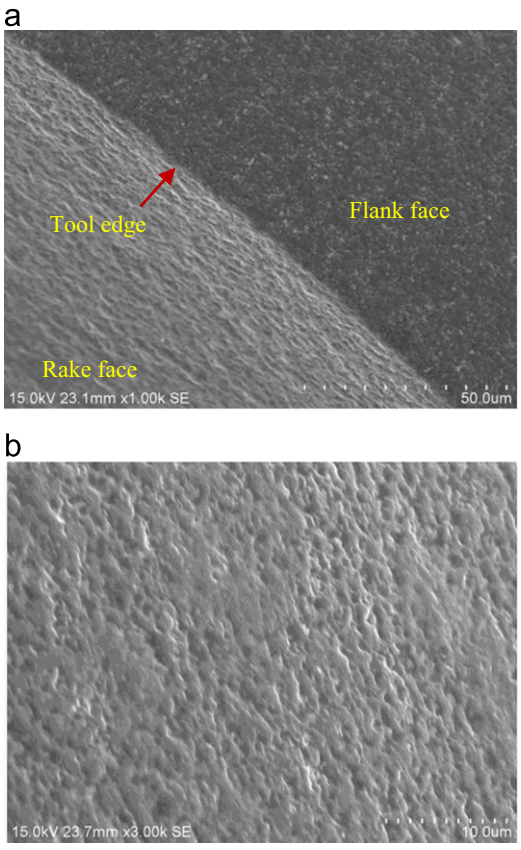

Fig. 9. SEM micrographs of (a) tool edge and (b) tool flank face in fine machining.

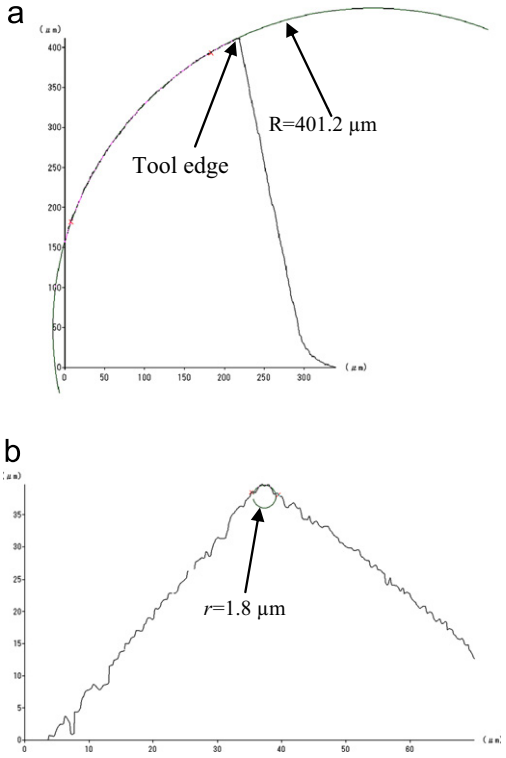

Fig. 10. Tool profile measurement results: (a) radius of flank face, (b) edge radius.

the tool surface turns to be distinctly smooth without deep craters. This indicates that diamond grains have been gradually removed layer by layer through graphitization rather than grain dislodgments.

The tool profile measurement results are shown in Fig. 10. As shown in Fig. 10(a), the radius of the spherical surface (flank face) is 401.2 μm, very close to the designed value (400 μm). In Fig. 10(b), the edge radius of the end mill is about 1.8 μm. These results for the first time demonstrated that one micron level form accuracy and edge sharpness is producible in EDM fabrication of PCD tools under optimized conditions. In addition, the average surface roughness of

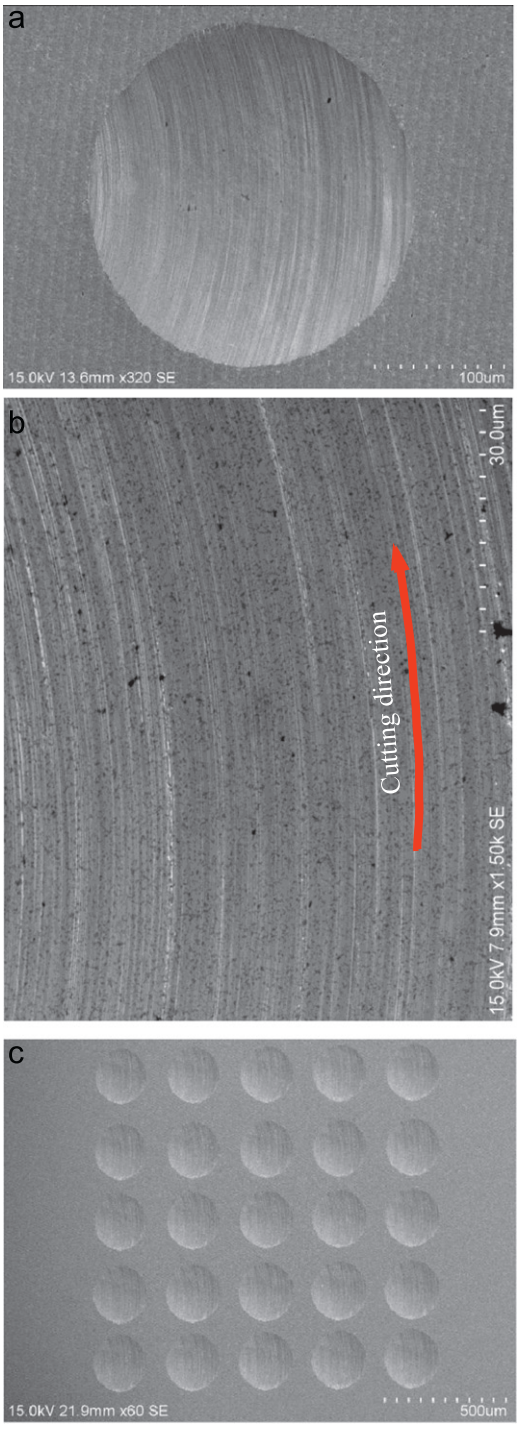

Fig. 11. SEM micrographs of machined micro dimples: (a) a single dimple, (b) magnified view of dimple surface, and (c) dimple array.

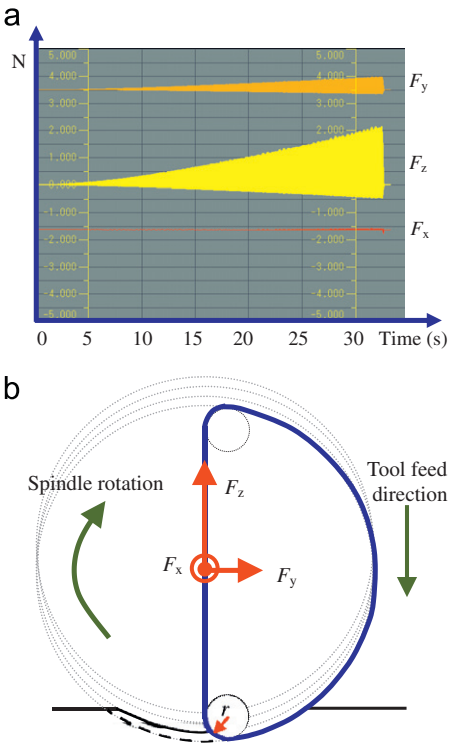

Fig. 12. Cutting forces in dimple machining: (a) force measurement results, (b) force model.

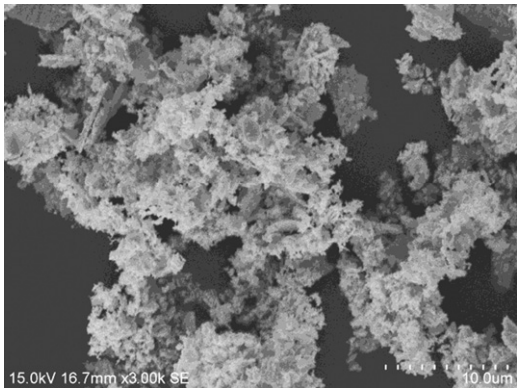

Fig. 13. SEM micrograph of the chips in end milling of tungsten carbide.

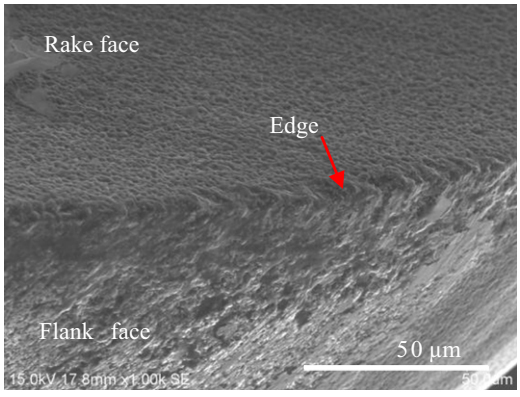

Fig. 14. SEM micrograph of tool edge after machining of 55 dimples on tungsten carbide.

tool rake face and tool flank face was 0.186 μm R_a (0.824 μm R_z), which is comparable to that obtained by fine grinding [13].

3.3. Micro machining tests on WC

The above EDM fabricated end mills were then used for cutting micro dimples on a WC mold substrate. Fig. 11(a) shows an SEM micrograph of a single dimple. The boundary between the dimple surface and the uncut surface is very clear, and there are slight tool marks along the cutting direction. Fig. 11(b) is a magnified view of the dimple surface. No brittle fractures can be found, thus we can say that the dimple surface has been machined in a ductile mode. Fig. 11(c) shows an SEM micrograph of a fabricated dimple array. All the 25 dimples are uniformly generated.

Fig. 12(a) shows variation of cutting forces during machining a single dimple. It can be seen that three force components (tangential F_y, thrust force F_z, and lateral force F_x) changes very stably as depth of cut increases. The forces increase with depth of cut because the cutting width, namely the effective contact length between the tool and the workpiece, increases with the dimple depth. It is also noticed that the thrust force (F_z) is significantly larger than the tangential force (F_y). This effect might be induced by the high contact pressure between the flank face and machined surface, as schematically shown in Fig.12(b).

Fig. 13 shows an SEM micrograph of the cutting chips. The chips are composed of extremely thin slices, indicating that shear deformation dominated material removal in machining. Because end milling is an intermittent process, the chips are extremely short, different from those long and continuous chips in diamond turning [38]. Fig. 14 shows an SEM micrograph of the cutting edge after machining 55 dimples. A slight flank wear can be found near the cutting edge, but edge chippings are too small to be recognized. This kind of wear characteristic is distinctly different from that of single crystalline diamond end mills [12].

It should be pointed out that the surface roughness of the machined dimple in Fig. 11 is quite rough. This is because the unevenness of the cutting edge was directly imprinted on the workpiece surface. Surface roughness can be improved by cross feeding the tool. This effect can be achieved by either rotating the workpiece along the dimple center or swing the tool surface vertically to the cutting direction. Unfortunately, these operations were not currently supported by the present experimental setup of the authors.

To demonstrate the effect of tool cross feeding, we performed micro grooving tests on a WC mold substrate. Fig. 15 is a schematic model for surface generation in micro grooving. As the tool feed direction is perpendicular to the cutting direction, when using a small tool feed, the unevenness of the tool edge will

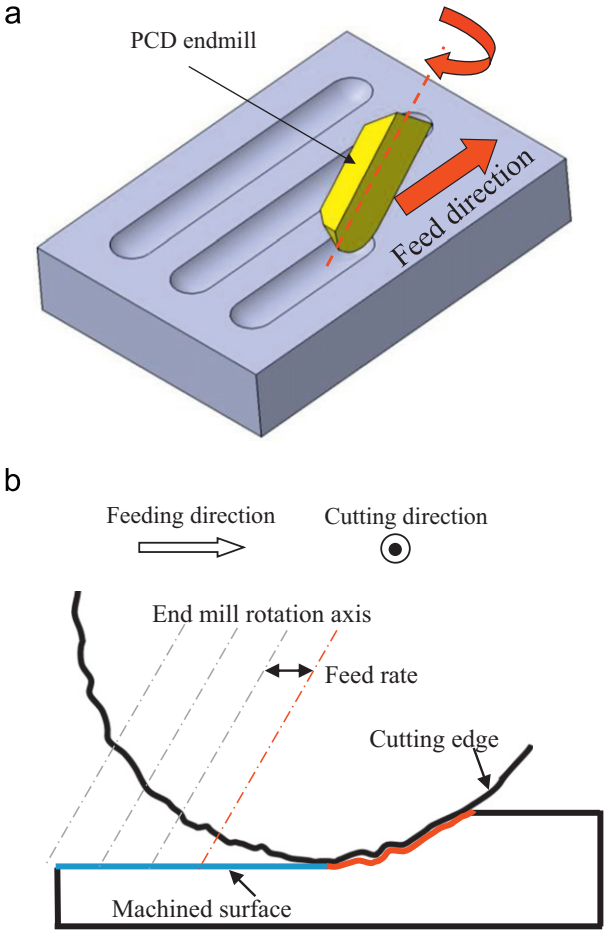

Fig. 15. Schematic of (a) micro grooving process and (b) surface generation mechanism.

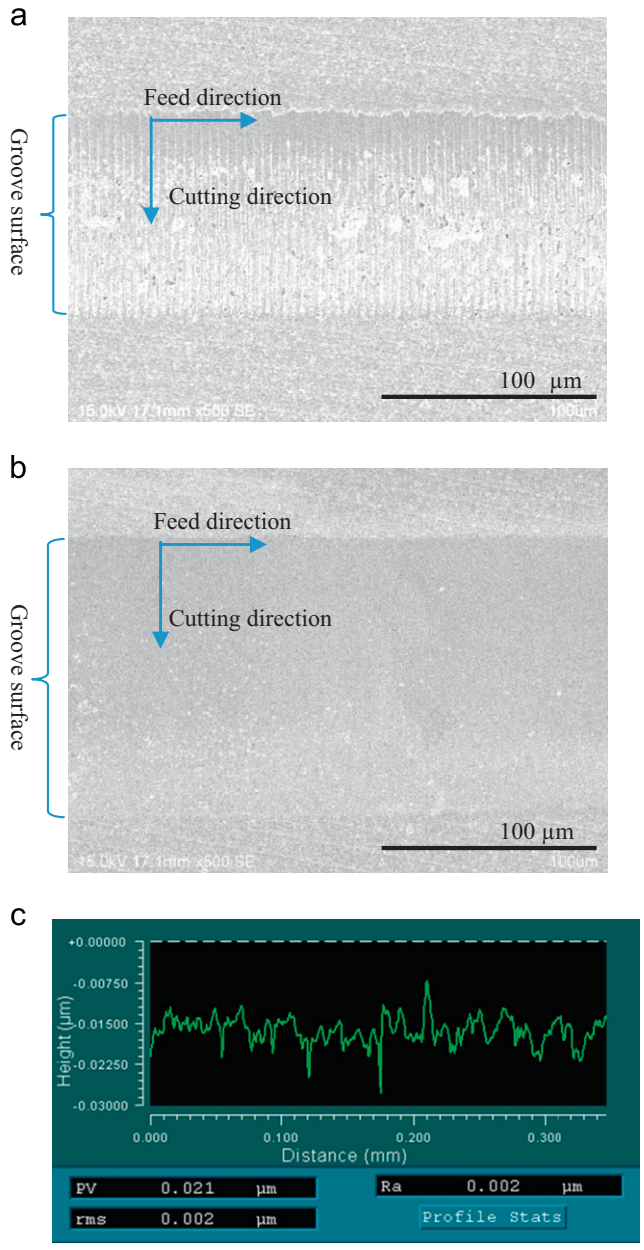

Fig. 16. SEM micrographs of groove surfaces machined at feed rates of (a) f=40 mm/min and (b) f=0.5 mm/min; (c) is the surface profile of (b).

not be imprinted on the machined surface. In this case, the finished surface can be far smoother than that of the cutting edge itself. Fig. 16(a) and (b) shows SEM micrographs of micro grooves machined at different tool feed rates. At a high feed rate (40 mm/min), significant feed marks and brittle fractures are seen on the grooved surface, while at a low feed rate (0.5 mm/min), the finished surface is extremely smooth without any visible feed marks and micro fractures. The groove surface roughness in this case is 2 nm R_a (21 nm R_y), as shown in Fig. 16(c). The surface quality is comparable to a fine polished surface. Therefore, EDM fabricated micro end mills can be used for high-precision micro machining of super hard mold materials for various kinds of functional microstructures.

4. Conclusions

Polycrystalline diamond end mills were fabricated by micro EDM, and the EDM mechanisms of PCD were investigated. The cutting performance of the fabricated tool was evaluated by machining microstructures on tungsten carbide. The following conclusions have been drawn:

(1) Diamond undergoes surface graphitization in EDM of PCD. The graphitization enables gradual removal of diamond instead of grain dislodgements, which is essential for improving tool sharpness and surface quality.
(2) Extremely low electro discharge energy conditions can be realized by using the stray capacitance of a RC circuit instead of using condensers.
(3) One micron level form accuracy and edge sharpness is producible in EDM fabrication of PCD tools under optimized conditions, and the surface roughness of tool face is comparable to that obtained by fine grinding.
(4) The fabricated end mills can be applied to fabricating high precision dimples and grooves on tungsten carbide. A smooth surface of 2 nm R_a, which is comparable to a polished surface, was achieved by ductile machining.
(5) A hybrid machining effect takes place in machining using the EDM fabricated PCD tools, which involves a cutting effect by tool rake face and a grinding effect by tool flank face.
(6) Edge micro chippings of a PCD end mill were distinctly fewer than those of a single crystalline diamond end mill when machining tungsten carbide.

References

[1] C. Evans, J. Bryan, "Structured", "Textured" or "Engineered" surfaces, CIRP Annals—Manufacturing Technology 48 (1999) 541–556.
[2] P. Nussbaum, R. Volkel, H. Herzig, M. Eisner, S. Haselbeck, Design, fabrication and testing of microlens arrays for sensors and microsystems, Pure and Applied Optics 6 (1997) 617–636.
[3] C. Pan, C. Su, Fabrication of gapless triangular microlens array, Sensors and Actuators A 134 (2007) 631–640.
[4] Noriaki Miura, Yuuki Noto, Shuusuke Kato, et al., Solar adaptive optics system at the Hida observatory, Proceedings of SPIE 7015 (2008) 70156U.
[5] L.A. Dobrzanski, A. Drygala, Surface texturing of multicrystalline silicon solar cells, Journal of Achievements in Materials and Manufacturing Engineering 31 (1) (2008) 77–82.
[6] D. Yu, G. Hong, Y. Wong, Profile error compensation in fast tool servo diamond turning of micro-structured surfaces, International Journal of Machine Tool and Manufacturing 52 (1) (2012) 13–23.
[7] E. Uhlmann, S. Piltz, K. Schauer, Micro milling of sintered tungsten-copper composite materials, Journal of Materials Processing Technology 167 (2005) 402–407.
[8] X. Rusnaldy, T. Ko, H. Kim, Micro-end-milling of single-crystal silicon, International Journal of Machine Tools and Manufacture 47 (2007) 2111–2119.
[9] W. Jung, Y. Heo, G. Yoon, K. Shin, S. Chang, G. Kim, M. Cho, Micro machining of injection mold inserts for fluidic channel of polymeric biochips, Sensors 7 (8) (2007) 1643–1654.
[10] M. Jahan, M. Rahman, Y. Wong, A review on the conventional and micro-electrodischarge machining of tungsten carbide, International Journal of Machine Tools and Manufacture 51 (12) (2011) 837–858.
[11] H. Weule, V. Hüntrup, H. Tritschler, Micro-cutting of steel to meet new requirements in miniaturization, CIRP Annals–Manufacturing Technology 50 (2001) 61–64.
[12] J. Yan, Z. Zhang, T. Kuriyagawa, H. Gonda, Fabricating micro-structured surface by using single-crystalline diamond endmill, The International Journal of Advanced Manufacturing Technology 51 (9-12) (2010) 957–964.
[13] P. Tso, Y. Liu, Study on PCD machining, International Journal of Machine Tools and Manufacture 42 (3) (2002) 331–334.
[14] K. Ho, S. Newman, State of the art electrical discharge machining (EDM), International Journal of Machine Tools and Manufacture 43 (13) (2003) 1287–1300.
[15] N.M. Abbas, D.G. Solomon, M.F. Bahari, A review on current research trends in electrical discharge machining (EDM), International Journal of Machine Tools and Manufacture 47 (7–8) (2007) 1214–1228.
[16] H. Nakaoku, T. Masuzawa, M. Fujino, Micro-EDM of sintered diamond, Journal of Materials Processing Technology 187–188 (2007) 274–278.
[17] T. Masuzawa, M. Fujino, K. Kobayashi, T. Suzuki, N. Kinoshita, Wire electro-discharge grinding for micro-machining, CIRP Annals–Manufacturing Technology 34 (1) (1985) 431–434.
[18] G. Chern, Y. Wu, J. Cheng, J. Yao, Study on burr formation in micro-machining using micro-tools fabricated by micro-EDM, Precision Engineering 31 (2) (2007) 122–129.
[19] J. Fleischer, T. Masuzawa, J. Schmidt, M. Knoll, New applications for micro-EDM, Journal of Materials Processing Technology 149 (2004) 246–249.
[20] J. Yan, K. Uchida, N. Yoshihara, T. Kuriyagawa, Fabrication of micro end mills by wire EDM and some micro cutting tests, Journal of Micromechanics and Microengineering 19 (2) (2009) 025004.
[21] K. Egashira, S. Hosono, S. Takemoto, Y. Masao, Fabrication and cutting performance of cemented tungsten carbide micro-cutting tools, Precision Engineering 35 (4) (2011) 547–553.
[22] T. Masaki, T. Kuriyagawa, J. Yan, N. Yoshihara, Study on shaping spherical poly crystalline diamond tool by micro-electro-discharge machining and micro-grinding with the tool, International Journal of Surface Science and Engineering 1 (4) (2007) 344–359.
[23] H. Minami, K. Watanabe, K. Masui, N. Nabekura, Electrical discharge truing for sintered polycrystalline diamond tool, Journal of the Japan society of electrical machining engineers 44 (105) (2010) 17–24.
[24] P. Koshy, V.K. Jain, G.K. Lal, Mechanism of material removal in electrical discharge diamond grinding, International Journal of Machine Tools and Manufacture 36 (10) (1996) 1173–1185.
[25] B. Yan, F. Huang, H. Chow, J. Tsai, Micro-hole machining of carbide by electric discharge machining, Journal of Materials Processing Technology 87 (1999) 139–145.
[26] O.N. Breusov, V.N. Drobishev, G.E. Ivanchihina, Effect of high temperature vacuum annealing on properties of detonation synthetic diamond, Proceedings of International Symposium on Physico-chemical Properties of Ultra-hard Materials, Academy of Science, Kiev, (1987) 48–53.
[27] D.V. Fedoseev, V.L. Buhovets, S.P. Vnukov, Graphitization of diamond at high temperatures, surfacial and thermo-physical properties of diamond, Proceedings of International Symposium on Physicochemical Properties of Ultra-hard Materials, Academy of Science, Kiev, (1985) 6–9.
[28] C. Everson, P. Molian, Fabrication of polycrystalline diamond microtool using a Q-switched Nd:YAG laser, The International Journal of Advanced Manufacturing Technology 45 (2009) 521–530.
[29] J. Qian, C. Pantea, J. Huang, T.W. Zerda, Y. Zhao, Graphitization of diamond powders of different sizes at high pressure-high temperature, Carbon, 42(12–13), 2691-2697.
[30] M.R. Patel, M.A. Barrufet, P.T. Eubanks, D.D. Dibitonto, Theoretical models of the electrical discharge machining process—the anode erosion model, Journal of Applied Physics 66 (9) (1989) 4104–4111.
[31] S.H. Yeo, W. Kurnia, P.C. Tan, Electro-thermal modeling of anode and cathode in micro-EDM, Journal of Physics D: Applied Physics 40 (8) (2007) 2513–2521.
[32] Nagahanumaiah, J. Ramkumar, N. Glumac, S.G. Kapoor, R.E. DeVor, Characterization of plasma in micro-EDM discharge using optical spectroscopy, Journal of Manufacturing Processes 11 (2009) 82–87.
[33] A. Kojima, W. Natsu, M. Kunieda, Spectroscopic measurement of arc plasma diameter in EDM, Annals of CIRP 57 (1) (2008) 203–207.
[34] W. Natsu, S. Ojima, T. Kobayashi, M. Kunieda, Temperature distribution measurement in EDM arc plasma using spectroscopy, JSME International Journal C 47 (1) (2004) 384–390.
[35] J. Sung, J. Lin, Diamond Nanotechnology: Synthesis and Applications, Pan Stanford Publishing, Singapore, 2009.
[36] M. Akaishi, H. Kanda, Y. Sato, N. Setaka, T. Ohsawa, O. Fukunaga, Sintering behaviour of the diamond-cobalt system at high temperature and pressure, Journal of Materials Science 17 (1982) 193–198.
[37] M.H. Nazare, A.J. Neves, Properties, growth and applications of diamond, INSPEC, IEE, London, 2001.
[38] J. Yan, Z. Zhang, T. Kuriyagawa, Mechanism for material removal in diamond turning of reaction-bonded silicon carbide, International Journal of Machine Tools and Manufacture 49 (5) (2009) 366–374.